

# The histone demethylase PHF8 is a molecular safeguard of the IFN $\gamma$ response

Elena Asensio-Juan<sup>1,†</sup>, Raquel Fueyo<sup>1,†</sup>, Stella Pappa<sup>1</sup>, Simona Iacobucci<sup>1</sup>, Carmen Badosa<sup>1</sup>, Sergi Lois<sup>2</sup>, Miriam Balada<sup>1</sup>, Laia Bosch-Presegué<sup>3</sup>, Alex Vaquero<sup>3</sup>, Sara Gutiérrez<sup>5</sup>, Carme Caelles<sup>4</sup>, Carme Gallego<sup>5</sup>, Xavier de la Cruz<sup>2,6</sup> and Marian A. Martínez-Balbás<sup>1,\*</sup>

<sup>1</sup>Department of Molecular Genomics, Instituto de Biología Molecular de Barcelona (IBMB), Consejo Superior de Investigaciones Científicas (CSIC), Barcelona 08028, Spain, <sup>2</sup>Vall d'Hebron Institute of Research (VHIR), Passeig de la Vall d'Hebron, 119, E-08035 Barcelona, Spain, <sup>3</sup>Chromatin Biology Laboratory, Cancer Epigenetics and Biology Program (PEBC), Institut d'Investigació Biomèdica de Bellvitge (IDIBELL), 08907- L'Hospitalet de Llobregat, Barcelona, Spain, <sup>4</sup>Department of Biochemistry and Molecular Biology, School of Pharmacy, University of Barcelona, Barcelona 08028, Spain, <sup>5</sup>Department of Cell Biology, Instituto de Biología Molecular de Barcelona (IBMB), Consejo Superior de Investigaciones Científicas (CSIC), Barcelona 08028, Spain and <sup>6</sup>Institut Català per la Recerca i Estudis Avançats (ICREA), Barcelona 08018, Spain

Received May 5, 2016; Revised December 19, 2016; Editorial Decision December 21, 2016; Accepted January 12, 2017

## ABSTRACT

**A precise immune response is essential for cellular homeostasis and animal survival. The paramount importance of its control is reflected by the fact that its non-specific activation leads to inflammatory events that ultimately contribute to the appearance of many chronic diseases. However, the molecular mechanisms preventing non-specific activation and allowing a quick response upon signal activation are not yet fully understood. In this paper we uncover a new function of PHF8 blocking signal independent activation of immune gene promoters. Affinity purifications coupled with mass spectrometry analysis identified SIN3A and HDAC1 corepressors as new PHF8 interacting partners. Further molecular analysis demonstrated that prior to interferon gamma (IFN $\gamma$ ) stimulation, PHF8 is bound to a subset of IFN $\gamma$ -responsive promoters. Through the association with HDAC1 and SIN3A, PHF8 keeps the promoters in a silent state, maintaining low levels of H4K20me1. Upon IFN $\gamma$  treatment, PHF8 is phosphorylated by ERK2 and evicted from the promoters, correlating with an increase in H4K20me1 and transcriptional activation. Our data strongly indicate that in addition to its well-characterized function as a coac-**

**tivator, PHF8 safeguards transcription to allow an accurate immune response.**

## INTRODUCTION

The immune system is responsible for detecting and combating pathogens. Once they are recognized, the immune response is activated, triggering the transcription activation of genes encoding cytokines, interferons and other antimicrobial proteins that allow a proper response (1,2). Type I and II interferons activate signaling pathways such as JAK/STAT and MAPK and have been identified as essential to counteract bacterial and viral infection (3,4). In particular, upon interferon gamma (IFN $\gamma$ ) signaling activation, STAT1 becomes phosphorylated, enters the nucleus and regulates the activation of pro-inflammatory gene promoters (5). A tight control of these cellular processes is crucial to avoid the appearance of inflammatory-related diseases such as type 2 diabetes (6), atherosclerosis (7) or neurodegenerative diseases (8). Cells have therefore developed mechanisms that prevent non-specific activation, that allow them to respond quickly upon signal activation and to return to a silent state when the stimulus finishes. However, the molecular mechanisms governing each of these steps are not fully understood.

Several studies have demonstrated that a subset of genes that respond to inflammatory signals are maintained in a repressive state prior to stimulation thanks to the action of corepressor complexes containing NCOR, SMRT and COREST (9–13). More recently, a new mechanism regu-

\*To whom correspondence should be addressed. Tel.: +34 93 403 4961; Fax: +34 93 403 4979; Email: mmbbmc@ibmb.csic.es

<sup>†</sup>These authors contributed equally to the paper as first authors.

Present address: Sergi Lois, Sistemas Genómicos de Valencia. Ronda G. Marconi, 6.46980 Paterna (Valencia).

lated by changes in the levels of histone 4 lysine 20 trimethylation (H4K20me3) has also been proposed (14). Glass *et al.* have demonstrated that SMYD5, a histone methyltransferase that specifically trimethylates H4K20me3, represses a subset of the pro-inflammatory promoters. The activation of these genes correlates with the demethylation of H4K20me3 by the Jumonji-containing histone demethylase (HDM) PHF2.

Histone 4 lysine 20 methylation (H4K20me) has been associated with DNA transcription, repair and compaction, depending on the grade of methylation (15). In particular, histone 4 lysine 20 monomethylation (H4K20me1) is enriched at the coding region of active genes, although it is also associated with chromatin compaction during mitosis (15,16). PHF8 is the only HDM responsible for demethylating H4K20me1 (17,18). In doing so, PHF8 regulates cell cycle progression (17,19). PHF8 is also necessary for the expression of many genes (18), including cell-cycle genes (17), Notch1-responsive genes (20) and cell structure genes (21). Importantly, deletions and point mutations in the PHF8 Jumonji-C (JmjC) catalytic domain lead to autistic spectrum disorders (ASDs) and Siderius-Hamel syndrome (22–27). In addition to the JmjC domain, PHF8 contains a PHD domain that recognizes and binds to nucleosomes trimethylated at lysine 4 in histone H3 (H3K4me3) and that are predominantly present at the transcription start site regions (TSS) of active promoters (28–33). H4K20me1 has been associated with both transcriptional activation and repression (16,34), highlighting the possibility that, in addition to being an activator, PHF8 could function as a transcriptional repressor. A recent *in silico* study proposed a potential role of PHF8 in corepressing genes together with REST/NRSF (35). However, the role of PHF8 in silencing transcription has not yet been molecularly described.

In this research article we investigate the function of PHF8 in maintaining the transcriptional silent state of IFN $\gamma$ -responsive genes. Analysis of microarray data revealed that after PHF8 depletion, a subset of inflammatory genes becomes upregulated. Further molecular studies indicated that PHF8 safeguards promoters to prevent signal-independent activation. Once the immune signal is triggered, PHF8 is evicted from the promoters, which correlates with the full activation of these genes. All together, our data indicate that PHF8 silences gene promoters to allow a precise gene response. Moreover, our data demonstrate how PHF8 displacement from IFN $\gamma$ -gene promoters leads to changes in the chromatin landscape that boost transcriptional activation.

## MATERIALS AND METHODS

### Cell culture, transfections and CoIP assays

HeLa S3, 293T, K562 cells were grown under standard conditions (36). Transfections were performed with calcium phosphate in the case of 293T cells and we used Fugene (Promega, E2691) for HeLa S3. Co-immunoprecipitation (CoIP) experiments with transfected proteins were carried out as described elsewhere (37).

### Plasmids and recombinant proteins

Lentiviral vectors were purchased from Sigma, brackets indicate target sequence: pLKO-hPHF8 (GCAGGTAATGGGAGAGGTT), pLKO-hHDAC (GCCGGTCATGTCCAAAGTAAT), pLKO-hSin3A (CCCTGAGTTGTTTAATTGGTT), pLKO-hERK2 (TGGAATTGGATGACTTGCCTA), pLKO-hERK1 (CCTGAATTGTATCATCAACAT) and pLKO-random (CAACAAGATGAAGAGCACC). pSuper vector with a nonspecific sequence (GGCTGAATGCAAGCGTGGA) or one specific to the human PHF8 sequence (GAGGAGAAGGCTGCTGACA). pEF6-PHF8-HA was kindly provided by Dr Christoph Loenarz. N-terminal-GST-mPHF8 (1-410) (N-terminal) was made by digesting pcDNA3-mPHF8 plasmid with EcoRV and HindIII restriction endonucleases, purification of the fragment and cloned into pGEX. Central-GST-mPHF8 (410-580) and C-terminal-GST-mPHF8 (590-733) were made following the same scheme but they were digested with HindIII or EcoRI restriction endonucleases respectively. Recombinant proteins were expressed in *Escherichia coli* as previously described (38). ERK's phosphatase expressing plasmid pSG5-MKP-1 and pcDNA3-HDAC1-FLAG are described elsewhere (36,39); pcDNA3-HA-ERK2 was obtained from Addgene (plasmid # 8974) (40); pCIG-mPHF8 is detailed in (21). The C-terminal-GST-mPHF8 mutant at the S614>A was generated using the QuickChange II XL Site-Directed Mutagenesis kit (Stratagene) with the following pair of primers AGTGCTGGGGGCGGCTGGGGCCT and AGGCCCCAGCCGCCCCAGCACT. The pEF6-hPHF8-HA S751>A mutant was generated likewise from pEF6-hPHF8-HA vector using GAGTGCTGGGAGCAGCTGGGGCCTC and GAGGCCCCAGCTGCTCCCAGCACTC as mutagenesis primers.

### Antibodies and reagents

Antibodies used were anti: PHF8 (Abcam ab36068), HA (Abcam 20084), FLAG M2 (Sigma F3165), MYC (Abcam ab9132),  $\beta$ -tubulin (Millipore MAB3408), H4K20me1 (Abcam ab9051), H4K20me3 (Abcam ab9053), H3K4me3 (Abcam ab8580), H3K9me2 (Abcam ab1220), HDAC1 (Abcam ab7028), SIN3A (K-20) (Santa Cruz Biotechnology), ERK2 (D-2) (Santa Cruz Biotechnology sc-1647) and ERK1 (K23) (Santa Cruz Biotechnology sc-94). Human recombinant IFN $\gamma$  was used at 5 ng/ml and purchased from Peprotech.

### Pull-down assays

Transfected cells were lysed in cold lysis buffer containing (25 mM Hepes, pH 7.5, 1% NP40, 0.25% (w/v) sodium deoxycholate, 10% (v/v) glycerol, 1 mM ethylenediaminetetraacetic acid, 150 mM NaCl, 10 mM MgCl<sub>2</sub>, 1 mM Na<sub>3</sub>VO<sub>4</sub>, 25 mM NaF, 1 mM PMSF and 10  $\mu$ g/ml each of leupeptin, aprotinin, pepstatin A and trypsin inhibitor. Nucleus-free supernatants were incubated with GST-PHF8 on glutathione-Sepharose beads and analyzed by immunoblot as described previously (41).

### Immunoblotting

Immunoblotting was performed by standard procedures and results were visualized on an Odyssey Infrared Imaging System (Li-Cor). Immunoblot quantifications were carried out with ImageJ software.

### Indirect immunofluorescence

Cells were fixed for 20 min in 4% paraformaldehyde and permeabilized with phosphate buffered saline-triton 0.1%. Indirect immunofluorescence was performed as described previously (42).

### ChIP assays

Chromatin Immunoprecipitation (ChIP) assays were carried out using previously described procedures (43). Fixation with 1% formaldehyde was stopped by the addition of 0.125 M glycine. Sonication step was performed in a Bioruptor sonicator (to obtain ~500 bp fragments) and chromatin was used for each immunoprecipitation. The antibody–protein complex was captured using magnetic beads (Magna ChIP™ Protein A Magnetic Beads Millipore 16–661). After decrosslinking DNA was purified using phenol/chloroform extraction followed by ethanol precipitation. Lastly, ChIP DNA was analyzed by qPCR with SYBR Green (Roche) in a LightCycler 480 PCR system (Roche). Percentage of input was used for the quantification of the immunoprecipitated material with respect to the total starting chromatin.

### ChIP-seq data obtention and comparison

ChIP-seq data were downloaded from ENCODE (44) (Accessions of peaks used in this paper are specified in Supplementary Table S1). For Venn diagrams construction we selected peaks on promoters (–800 to +200 bp) and overlap them using Galaxy (45). ChIP-seq captions were obtained from UCSC genome browser.

### mRNA extraction and qPCR

TRIZOL reagent (Invitrogen) was used to extract mRNA, following the manufacturer instructions. Reverse transcription was performed with Transcriptor First Strand cDNA Synthesis Kit 200 reactions (Roche) and qPCR was performed with SYBR Green (Roche) in a LightCycler 480 (Roche) using specific primer pairs (See Supplementary Table S2).

### RNA-seq analysis

Accession numbers can be found in Supplementary Table S1. In brief, reads were mapped to the hg19 genome version using TOPHAT package (46). Transcript levels were calculated with Cufflink (47) and differentially expressed genes were identified with Cuffdiff (48).

### Tandem affinity purification

Tandem affinity purification (TAP) of PHF8 multiprotein complexes was performed in 293T cells expressing TAP-PHF8 as described in (49). Several bands visible from silver or comassie staining were cut out from the gel. The analysis of the interacting proteins was carried out by liquid chromatography/ mass spectrometry (LC/MS) in the Proteomics Unit of the ‘Institut de Recerca de la Vall d’Hebrón’ (Barcelona) using Mascot search engine to define significant hits.

### Lentiviral transduction

It was carried out as previously described (50). Basically, 293T cells growing in a 10-cm dish were transfected with a mix of packaging, envelop and shRNA transfer vector DNAs (6, 5 and 7 µg, respectively). After 30 h of transfection, medium was collected and virus concentrated by ultracentrifugation (26 000 rpm, 2 h at 4°C). Viral particles were then added to receptor cells. After 24 h, transduced cells were selected with puromycin (5 µg/ml). Finally, the efficiency of knockdown constructs was assessed by qPCR and immunoblot. Plasmids were purchased from Sigma.

### ERK2 kinase assay

Hemagglutinin-ERK2 was immunoprecipitated using anti-HA antibody from either IFN $\gamma$ , and untreated cells. ERK2 kinase activity was determined as described previously (51).

### Statistical analysis

All quantitative data from the shown experiments correspond to the mean and standard error of the mean (S.E.M.) of at least two independent biological replicates, being more frequent to carry out three or four independent experiments. Significant differences between groups were tested by Student’s *t*-test of paired samples and asterisks correspond to *P*-value 0.05 (\*), 0.01 (\*\*) and 0.001 (\*\*\*).

## RESULTS

### PHF8 interacts with co-repressors

PHF8 binds widely throughout the genome and targets many promoters. However, its presence does not always correlate with transcriptional activation (52). To gain further insight into the role of PHF8, we performed TAP using 293T cells expressing PHF8 fused to the TAP tag (TAP-PHF8) to identify new interacting partners. Some proteins that copurified in at least two experiments were identified by mass spectrometry. Peptides belonging to the general repressor SIN3A and the kinase ERK2 were found enriched in our sample as Mascot score points show (Figure 1A). SIN3A stably associates with HDAC1 and HDAC2 to form a well-characterized corepressor complex that also includes SAP30, SAP18, RBBP4 and RBBP7 (53,54). This complex can be recruited to promoters via interactions with sequence-specific transcription factors (55,56) to repress transcription (53,54,57). In addition, ERK2 has recently been described as a DNA binding protein that regulates genes involved in the IFN $\gamma$  signaling by recognizing



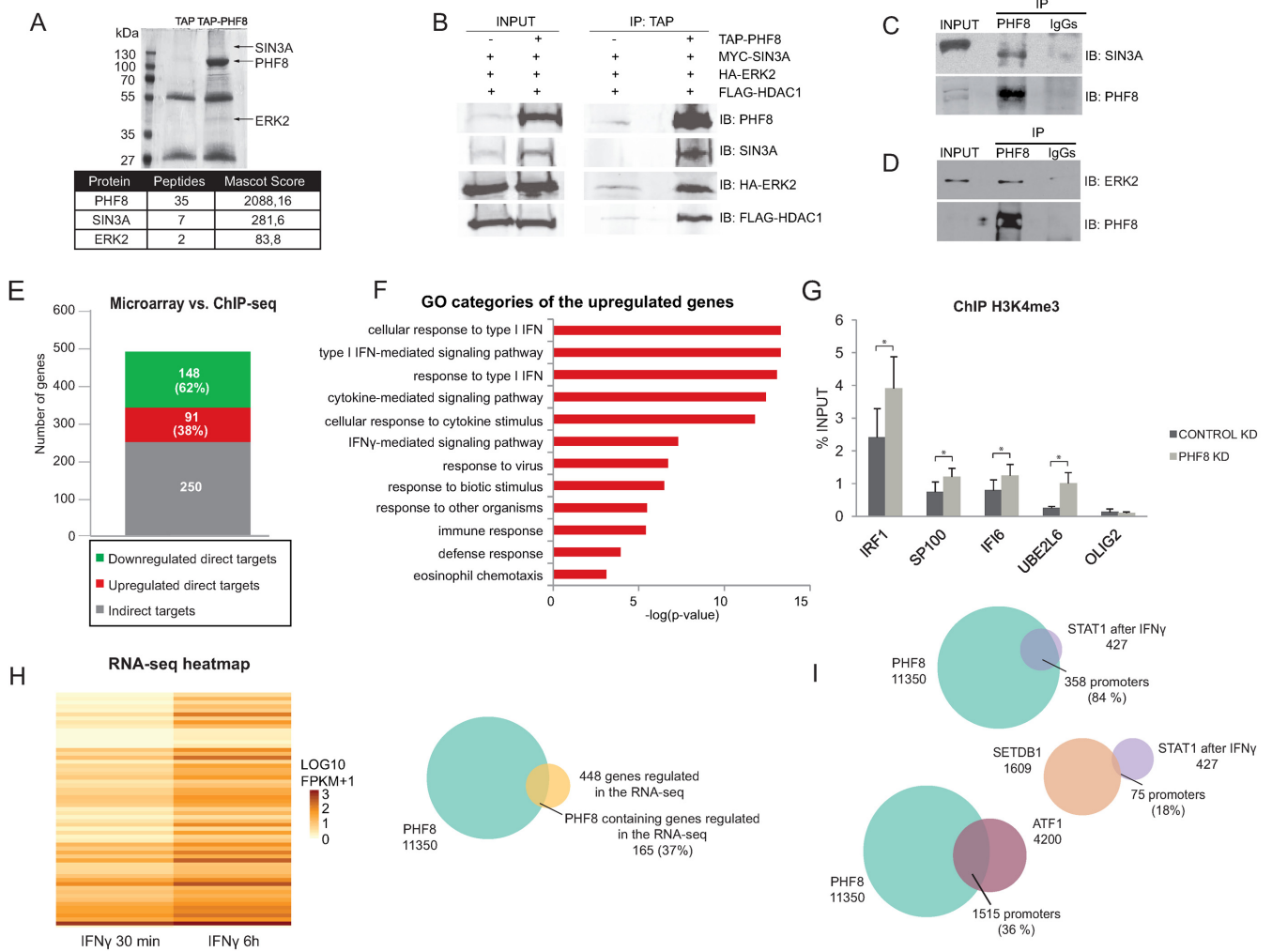


**Figure 1.** PHF8 interacts with corepressors. (A) TAP purification of PHF8 from transfected control (TAP, transfected with the vector alone) or over-expressing PHF8 (TAP-PHF8) 293T cells. After precipitation, PHF8 and associated polypeptides were loaded into a SDS-PAGE gel and stained with Coomassie blue. Some bands from the gel were cut out and identified by mass spectrometric analysis (indicated on the right) after subtraction of peptides that were present in control. Table indicates number of peptides and Mascot score for hits. (B) HeLa S3 cells were transfected with PHF8, ERK2, SIN3A or HDAC1 as indicated. PHF8 was precipitated using the TAP tag and the presence of SIN3A, HDAC1 and ERK2 in the immunopellet was determined by immunoblot with the antibodies indicated on the right. This is representative of at least three biological independent experiments. (C) HeLa S3 nuclear extracts were prepared and PHF8 was immunoprecipitated. The association with SIN3A in the immunopellet was revealed by immunoblot with the indicated antibodies. This depicts a representative of at least two biological independent experiments. (D) HeLa S3 cells were treated with IFN $\gamma$  (2h) and nuclear extracts were prepared. PHF8 was immunoprecipitated and the presence of ERK2 protein in the immunopellet was identified by immunoblot. Input represents 0.5% of the used extract. This depicts a representative of at least two biological independent experiments. (E) Diagram showing the number and percentage of PHF8 regulated genes [in a microarray using control or PHF8-depleted HeLa cells (21)] that are PHF8 direct targets determined in ChIP-seq experiments (21,52). (F) The PHF8-direct targets genes and upregulated in the microarray were analyzed with Gene Ontology tool. The chart shows the over-represented biological functions for upregulated genes. (G) H3K4me3 ChIP assay in CONTROL and PHF8 KD HeLa S3 cells analyzed by qPCR, at the TSS of the indicated genes. Percentage of input indicates the mean of at least three biological replicates. Error bars show standard deviation of the mean (S.E.M). For statistical analysis a paired-sample *t*-test was calculated, \**P* < 0.05. (H) RNA-seq heatmap showing the genes differentially regulated upon IFN $\gamma$  addition (comparing 30 min and 6h) to K562 cells (left panel). Diagram showing the number of genes differentially regulated upon IFN $\gamma$  addition that contain PHF8 bound to their promoter in untreated K562 cells (right panel). (I) Venn diagrams showing the number of promoters that contain overlapping (i) PHF8 peaks prior IFN $\gamma$  treatment and STAT1 peaks after IFN $\gamma$  addition (30 min) or (ii) STAT1 peaks after IFN $\gamma$  addition (30 min) and SETDB1 peaks prior IFN $\gamma$  treatment or (iii) PHF8 peaks prior IFN $\gamma$  stimulation and ATF1 peaks in K562 cells (data obtained from ENCODE, Supplementary Table S1).

and binding to the sequence C/GAAAC/G at promoters (58). To further understand the functional significance of these interactions, we first confirmed that PHF8 interacts with SIN3A, ERK2 and potentially HDAC1 by carrying out co-immunoprecipitation (CoIP) experiments with over-expressed proteins (Figure 1B and Supplementary Figure S1A) and with the endogenous proteins (Figure 1C and D). Next, we identified the PHF8 regions responsible for these interactions. To do that, we fragmented the 795 amino acid mouse PHF8 isoform into three regions: the N-terminal (1–410) containing the JmjC and PHD domains and the two CDK1-phosphorylation sites (17); the central region (410–580) and the C-terminal (590–733) fragment, which contains one CDK2-phosphorylation site and a serine-rich domain. Next, by pull-down assay, we determined the PHF8 region responsible for interaction with HDAC1 to be the N-terminal region containing the PHD and the JmjC domains (Supplementary Figure S1B). This region, as well as the C-terminal domain, also binds to ERK2 (Supplementary Figure S1C). These associations suggest that PHF8, besides its well-characterized function as a coactivator (59), might interact with corepressors to pause or silence transcription. To gain insight into this potential new function of PHF8, we re-examined the transcriptional profile previously determined in our laboratory, which compared control and PHF8-depleted HeLa cells by using an shRNA against PHF8 (21) and the PHF8 binding sites determined by ChIP-seq in the same cell line (52). We identified 91 up-regulated genes in PHF8-depleted cell line compared with control cells, representing 38% of the total direct targets of PHF8 [Figure 1E and (21)], alluding again to a potential role of PHF8 in preventing transcription activation. To gain further insight into the possibility that PHF8 works preventing transcription activation, we first determined the identity of the genes upregulated in the microarray experiment by assessing their molecular and cellular functions using the Gene Ontology tool (60). Interestingly, we found that among the enriched groups were many genes related to IFNs and immune response [Figure 1F (21)]. To rule out any possibility of shRNA off-target effects we performed the following experiments: we transiently transfected a random shRNA or the PHF8 shRNA and we stably knocked down PHF8 by transduction of lentiviral particles containing a second independent PHF8 shRNA. In both cases we checked by qPCR the expression of several IFN-responsive genes and by immunoblot the PHF8 protein levels. Results in Supplementary Figure S1D showed that the expression of the analyzed genes was affected independently of the used shRNA. Finally, over-expression of a resistant PHF8 (mPHF8) protein (21) in the stable PHF8 knock-down HeLa cells (that we called PHF8 KD), restored the expression of the majority of the analyzed genes (Supplementary Figure S1E). Secondly, we confirmed that upregulation of some IFN $\gamma$ -responsive genes in the PHF8 KD cells correlated with an increase in H3K4me3 levels, a histone mark that associates with transcriptional activation (Figure 1G). Thirdly, to analyze further the association between PHF8 and antiviral activity, we compared PHF8 genome-wide binding at promoters in basal conditions and the genes that respond to IFN $\gamma$  identified by RNA-seq in the lymphocytic cell line K562. From the 448 regulated

genes upon IFN $\gamma$  treatment ( $q$ -value < 0.05) 165 (37%) have PHF8 bound to their promoter before activation (Figure 1H). In order to understand this association, we compared PHF8 binding sites at promoters in basal conditions and STAT1 recruitment sites upon IFN $\gamma$  stimulation of K562 cells. The Venn diagrams in Figure 1I show that 84% of genes bound by STAT1 upon IFN $\gamma$  addition were previously bound by PHF8, while only 18% colocalized with SETDB1, a well-known and unrelated co-repressor. Moreover, only 36% of PHF8 binding sites also contain the unrelated activator ATF1, thus excluding the possibility of random colocalization. As expected, many of the analyzed IFN $\gamma$ -responsive genes were likewise upregulated in K562 cells upon PHF8 depletion (Supplementary Figure S2A). Altogether, these results indicate that PHF8 participates in IFN $\gamma$  gene regulation likely by interacting with corepressors.

### PHF8 displacement from IFN $\gamma$ -activated promoters correlates with transcriptional activation.

The previous data indicate that PHF8 binds IFN $\gamma$ -responsive gene promoters before signaling activation. To further understand the dynamics of PHF8 in response to IFN $\gamma$ , we analyzed, by ChIP-qPCR, the promoter occupancy of a subset of IFN $\gamma$  regulated-responsive promoters selected according to their appearance in both microarray and RNA-seq (*IRF1*, *SP100*, *IFI6* and *UBE2L6*), a non-IFN $\gamma$ -responsive but PHF8 target (*CTNNA1*) (21) and a non-PHF8 target (*OLIG2*) (Figure 2A). Upon IFN $\gamma$  treatment, binding of PHF8 to the TSS of the IFN $\gamma$  target genes decreased (Figure 2B). In contrast, its association with the *CTNNA1* promoter did not change (Figure 2B). No effect was observed in the PHF8 occupancy at the negative control gene *OLIG2* (Figure 2B). In agreement, PHF8 displacement from the *IRF1*, *SP100*, *IFI6* and *UBE2L6* promoters was concomitant with transcriptional activation of the corresponding genes (Figure 2C). Similar regulation was observed on K562 cells upon IFN $\gamma$  addition (Supplementary Figure S2B). Interestingly, the transcriptional response to IFN $\gamma$  was higher in PHF8 KD than in Control KD cells, as expected for the proposed role of PHF8 in preventing transcription activation (Supplementary Figure S3A). The PHF8-ChIP signals are specific as PHF8 immunoprecipitation in PHF8 KD cells did not generate any ChIP enrichment at the analyzed promoters (Supplementary Figure S3B). Neither PHF8 protein levels (Supplementary Figure S3C), its subcellular localization (Supplementary Figure S3D) nor the cell cycle phase distribution (Supplementary Figure S3E) were affected by IFN $\gamma$  treatment, confirming that PHF8 loss at the promoters is specific.

As PHF8 is the HDM responsible for H4K20me1 demethylation (17), we speculated whether this histone mark changed in coordinated fashion with the IFN $\gamma$ -mediated transcriptional response. We therefore performed ChIP assays, which detected a significant increase in H4K20me1 levels that correlated with PHF8 eviction from the promoters (Figure 2D). Moreover, a significant reduction in the H4K20me3 histone mark (Figure 2E) and an increase in H3K4me3 levels were observed (Figure 2F). None of these changes were detected at the non-responsive PHF8-

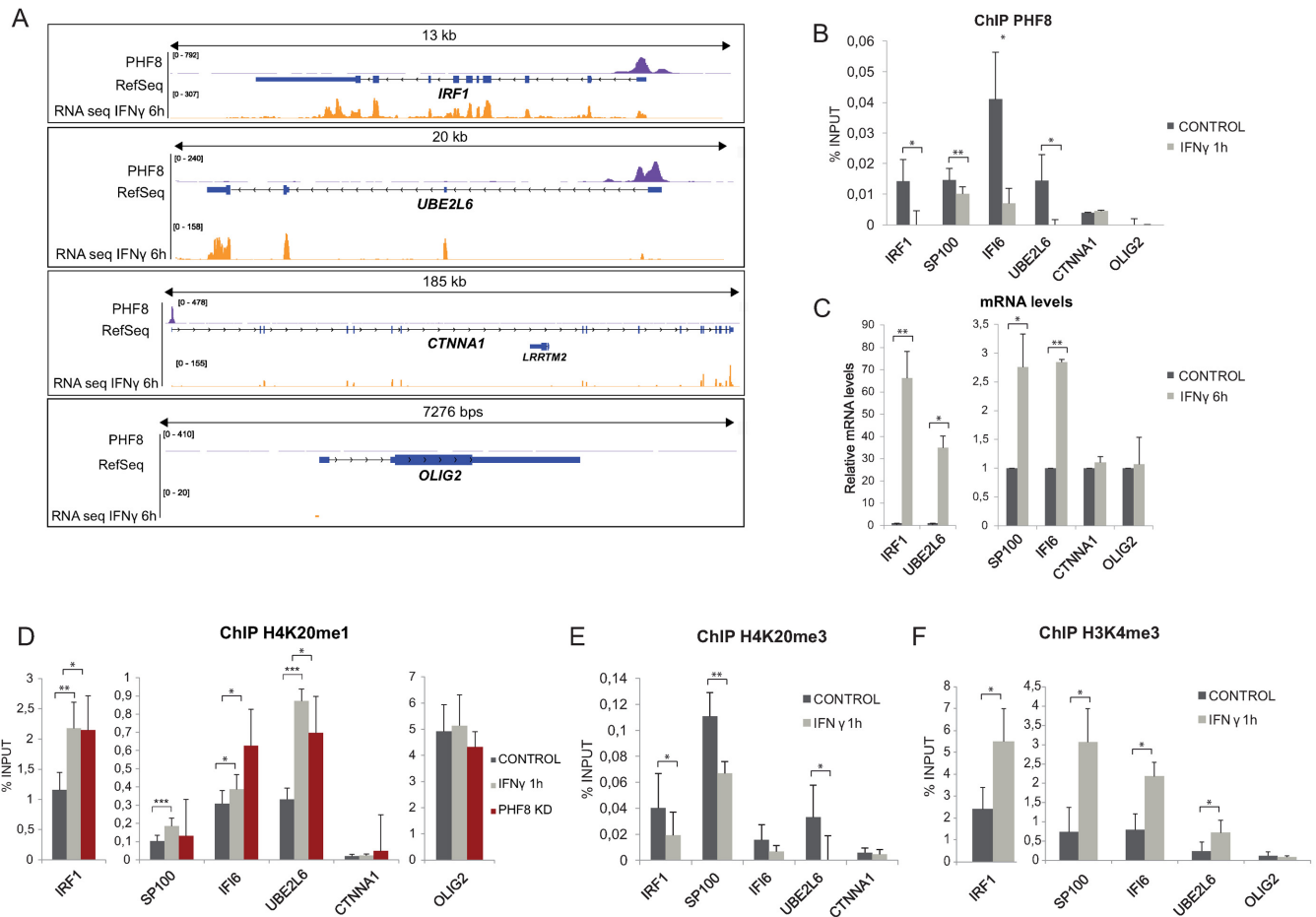


**Figure 2.** PHF8 displacement from IFN $\gamma$ -responsive promoters correlates with transcriptional activation. (A) Representation of the PHF8 ChIP-seq tracks prior IFN $\gamma$  treatment and RNA-seq upon IFN $\gamma$  stimulation in K562 cells. (B) ChIP of PHF8 in HeLa S3 cells analyzed by qPCR at the TSS of the indicated genes prior and upon IFN $\gamma$  treatment (1h). Results are the mean of three biological independent experiments. (C) mRNA levels of several PHF8-dependent and IFN $\gamma$ -responsive genes in HeLa S3 cells prior and upon IFN $\gamma$  treatment (6h) quantified by qPCR. Data were normalized to 18S mRNA levels. Results are the mean of three independent experiments. (D) H4K20me1 ChIP assay in CONTROL cells prior and upon IFN $\gamma$  treatment (1h) or in PHF8 KD HeLa S3 cells analyzed by qPCR at the TSS of the indicated genes. Percentage of input represents the mean of at least three biological independent experiments. (E and F) H4K20me3 (E) or H3K4me3 (F) ChIP assay in HeLa S3 cells prior and upon IFN $\gamma$  stimulation (1h). Samples were analyzed by qPCR at the TSS of the indicated genes. Results are the mean of three biological independent experiments. Error bars indicate S.E.M. For statistical analysis a paired-sample *t*-test was calculated, \* $P < 0.05$ ; \*\* $P < 0.01$ ; \*\*\* $P < 0.001$ .

target promoter (*CTNNA1*) or at the PHF8-binding negative control (*OLIG2*) (Figure 2D and F). Importantly, a clear increase in H4K20me1 levels prior to IFN $\gamma$  treatment was observed in KD PHF8 cells, suggesting that PHF8 was responsible for maintaining the low levels of H4K20me1 at *IRF1*, *SP100*, *IFI6* and *UBE2L6* promoters before signal activation (Figure 2D). In the same way PHF8 demethylates H4K20me1, this HDM is known to exert its function over H3K9me2 in other cellular contexts (52,61). Furthermore, H3K9me2 has been related to the IFN $\gamma$  response (62). We therefore analyzed the IFN $\gamma$  chromatin landscape by performing H3K9me2 ChIP experiments. Interestingly, a significant increase in H3K9me2 levels upon IFN $\gamma$  addition was observed (Supplementary Figure S3F). However, PHF8 is probably not involved in H3K9me2 demethylation at these promoters as no changes in H3K9me2 levels were observed in KD PHF8 cells (Supplementary Figure S3F).

In summary, these data demonstrate that PHF8 is evicted from the IFN $\gamma$ -regulated promoters upon signaling activa-

tion. This correlates with gene activation and changes in the promoters' chromatin status. In particular, we identified a switch between mono- and trimethylation at H4K20, H4K20me1 increases while H4K20me3 decreases upon IFN $\gamma$  stimulation. PHF8 might, thus, be preventing gene activation by maintaining an adequate balance of H4K20 methylation at the analyzed IFN $\gamma$ -responsive gene promoters.

### SIN3A-HDAC1 corepressors cooperate with PHF8 to prevent transcription activation

The previous data indicate that PHF8 plays a role in preventing IFN $\gamma$ -responsive gene activation by maintaining the balance of H4K20 methylation at the analyzed promoter regions (Figure 2). Furthermore, PHF8 interacts with the SIN3A-HDAC co-repressor complex (Figure 1). These observations provided us with the rationale to explore the possibility that, in addition to H4K20me1 demethyla-



tion, SIN3A complex might be cooperating with PHF8 to silence transcription. Interestingly, our genome-wide analysis indicated that 96% of the gene promoters bound by SIN3A and HDAC1 also bind PHF8 in K562 cells prior to IFN $\gamma$  activation (Figure 3A and B). To further understand the functional relevance of this association, we sought to determine whether HDAC1 and SIN3A contribute to silencing the IFN $\gamma$ -responsive genes in the absence of a signal. In order to do this, we established two cell lines that express low levels of SIN3A (SIN3A KD) or HDAC1 (HDAC1 KD), without affecting PHF8 levels (Figure 3C and Supplementary Figure S4A), [although an increase in HDAC2 was observed in HDAC1 KD cells (Supplementary Figure S4B)]. The expression of some PHF8-dependent IFN $\gamma$ -genes was assessed by qPCR. The results demonstrated that depletion of HDAC1 or SIN3A led to an increase in the levels of many of the genes analyzed (Figure 3C and Supplementary Figure S4A), suggesting that HDAC1 and SIN3A might cooperate with PHF8 to keep them silenced. To confirm this hypothesis, we tested the presence of HDAC1 and SIN3A at the analyzed promoters through the use of ChIP assays. Our data, shown in Figure 3D and E, revealed that, similarly to PHF8, HDAC1 and SIN3A were bound to the promoters prior to IFN $\gamma$  treatment. In order to better understand the interdependency between these factors, we have assayed the presence of PHF8 at the analyzed promoters in SIN3A KD and HDAC1 KD cells. Results show that PHF8 binding is partially lost in both cases, suggesting that these three cofactors influence each other's localization (Figure 3F and Supplementary Figure S4C). To confirm this hypothesis, we have also tested the SIN3A association to promoters in PHF8 KD cells, showing that SIN3A binding at the analyzed promoters decreases in PHF8 depleted cells (Figure 3G). Finally, we investigated the dynamics of the co-repressor complex after activation of the signal. HDAC1 ChIP results confirmed that HDAC1 was displaced from these promoters upon IFN $\gamma$  addition (Supplementary Figure S4D), probably together with PHF8 since the interaction between HDAC1 and PHF8 was maintained after IFN $\gamma$  signal activation (Supplementary Figure S4E).

Altogether, these data strongly suggest that PHF8 interacts with the SIN3A corepressor complex, which, in addition to H4K20me1 demethylation, contributes to preventing signal-independent activation of the IFN $\gamma$  genes.

### ERK2 regulates PHF8 chromatin binding affinity

It has been proposed that ERK2 binds IFN $\gamma$ -responsive promoters by recognizing the sequence C/GAAAC/G (58). To test for the presence of ERK2-consensus binding sites in our target promoters, we looked for evolutionary conserved promoter portions of at least 90% similarity and a minimum of 100 bp long in the online software Evolutionary Conserved Regions combined with rVista 2.0, a tool used to search for DNA binding proteins sites. Interestingly, we found the sequence in the previous mentioned promoters (Figure 4A). As PHF8 interacts with ERK2 (Figure 1) and, moreover, these have been proposed to co-occupy promoters in hESC (63), we hypothesized that ERK2 could be targeting PHF8 to IFN $\gamma$ -regulated promoters. To investigate this possibility, we first checked whether ERK2 is bound

to the analyzed promoters by employing ChIP assays. The data presented in Figure 4B indicate that ERK2 is associated with the IFN $\gamma$ -responsive promoters. Secondly, we assessed whether ERK2 affected PHF8 binding to these promoters. In order to do this, we established a HeLa S3 cell line that expresses low levels of ERK2 (ERK2 KD) (Supplementary Figure S5A) without affecting PHF8 (Supplementary Figure S5B) or ERK2 relative, ERK1, expression (Supplementary Figure S5A). We evaluated the binding of PHF8 by performing ChIP-qPCR. Strikingly, depletion of ERK2 led to an increase in PHF8 binding to the analyzed promoters in both basal and IFN $\gamma$ -stimulation conditions (Figure 4C). Moreover, ERK1/2 depletion partially blocked the IFN $\gamma$ -mediated transcriptional response of the analyzed genes (Figure 4D). Results clearly indicate that ERK2 is not responsible for PHF8 targeting on IFN $\gamma$ -responsive promoters, even though it is involved in PHF8 binding to chromatin. Next, we sought to investigate whether the catalytic activity of ERK was implicated in the observed effects on PHF8 binding. To do that, we overexpressed the ERK's phosphatase, MKP-1 (39), and analyzed the effects on the transcriptional response to IFN $\gamma$ ; data show attenuation of the IFN $\gamma$  response in the presence of the ERK's phosphatase (Figure 4E). Interestingly, the effects of MKP1 on transcription correlated with a clear increase of PHF8 binding at the analyzed promoters after IFN $\gamma$  addition (Figure 4F). These data suggest that ERK regulates PHF8's affinity to promoters in a catalytic dependent manner.

Since it has been previously described that PHF8 phosphorylation by CDK1 and CDK2 affects its ability to associate with chromatin (17,64), we therefore hypothesized that interaction with ERK2 might result in PHF8 phosphorylation. To test this possibility, we determined whether PHF8 was phosphorylated by ERK2 in response to IFN $\gamma$ . A close examination of the PHF8 protein sequence identified a highly conserved among species ERK2 phosphorylation site at amino acid 751 (human) and 614 (mouse) (Supplementary Figure S5C). Then, we performed a kinase assay with ERK2 purified from 293T cells stimulated or not with IFN $\gamma$ . Results presented in Figure 4G show a significant increase in the phosphorylation signal after IFN $\gamma$  treatment in mPHF8 C-terminal region, that contains the serine 614 putative ERK2 phosphorylation site. We did not detect any increase in the signal in mPHF8 N-terminal region or GST alone. Moreover, this increment in phosphorylation was lost in the mPHF8 C-terminus mutated at the conserved serine (S614A) (Supplementary Figure S5D and Figure 4H). In order to confirm that ERK2 is the enzyme responsible to this phosphorylation, we repeated the experiment upon IFN $\gamma$  treatment in the presence of MKP-1. Data show an almost complete abrogation of PHF8 phosphorylation in the presence of the ERK's phosphatase (Figure 4H). Finally, we sought to test whether the PHF8 phosphorylation mutant binds promoters upon IFN $\gamma$  stimulation. Results in Figure 4I demonstrate that this mutant, which is not efficiently phosphorylated upon IFN $\gamma$  signal, is bound to the promoters with higher affinity than PHF8 WT (Figure 4I). To discard any potential mislocalization of the overexpressed proteins we performed some immunofluorescence analysis that confirmed that both WT-PHF8 and S751A-

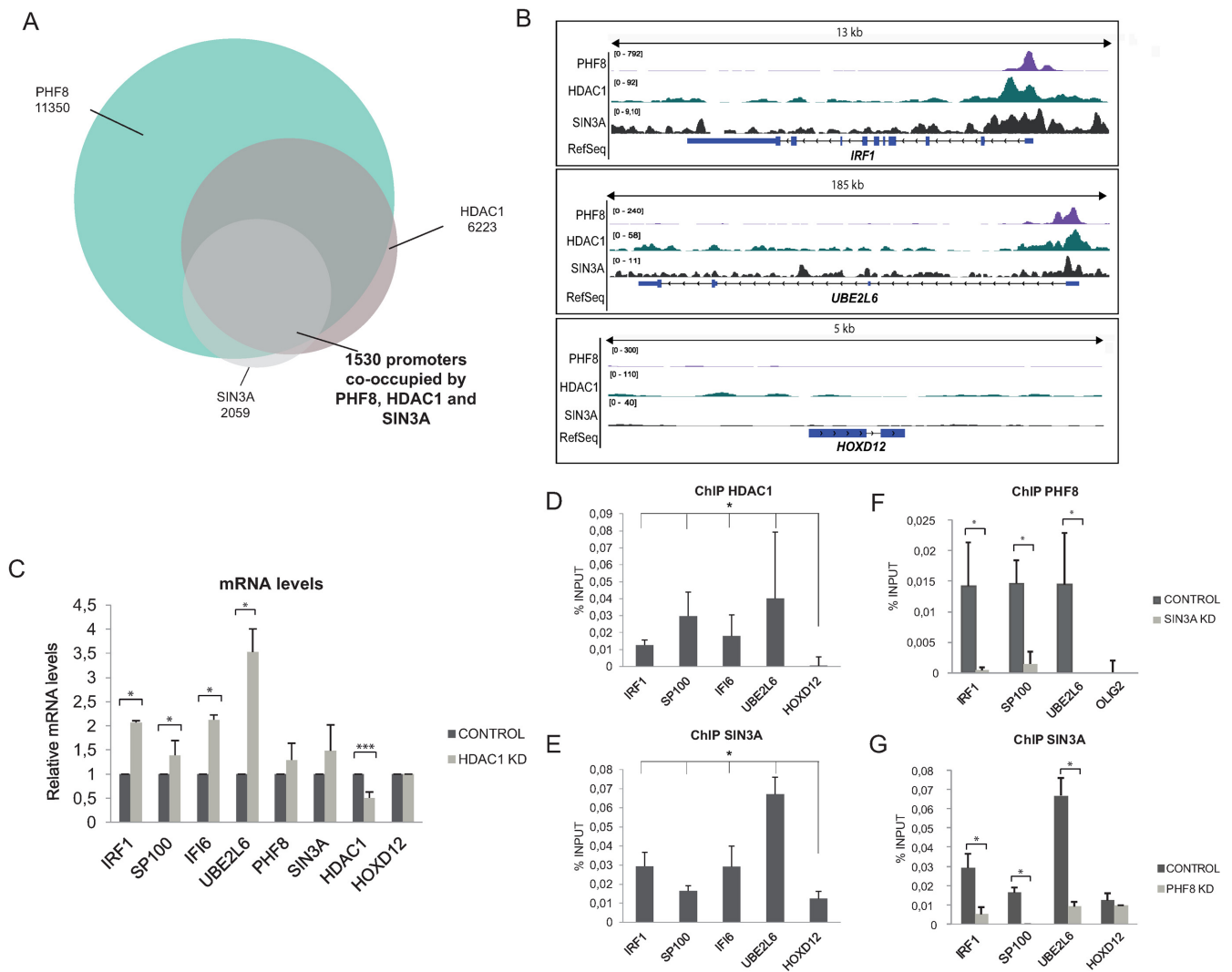


**Figure 3.** SIN3A–HDAC1 corepressor complex cooperates with PHF8 to prevent transcription activation. (A) Venn diagrams showing the number of PHF8, SIN3A and HDAC1 promoter overlapping peaks in untreated K562 cells (data obtained from ENCODE, Supplementary Table S1). (B) Representation of the ChIP-seq tracks for PHF8, HDAC1 and SIN3A at the indicated IFN $\gamma$ -responsive genes *IRF1* and *UBE2L6* and the negative control *HOXD12* in untreated K562 cells. (C) mRNA levels of several IFN $\gamma$  responsive genes in CONTROL and HDAC1 KD HeLa S3 cells quantified by qPCR. Data were normalized by 18S mRNA levels. Results are the mean of four biological independent experiments. (D and E) ChIPs of HDAC1 (D) or SIN3A (E) analyzed by qPCR at the promoter of several IFN $\gamma$ -responsive genes in HeLa S3 cells. Percentage of input represents the mean of at least three biological independent experiments. (F and G) ChIPs of PHF8 in HeLa S3 SIN3A KD cells (F) or ChIPs of SIN3A in HeLa S3 PHF8 KD cells (G) analyzed by qPCR. Percentage of input represents the mean of at least two biological independent experiments. Error bars indicate S.E.M. For statistical analysis a paired-sample *t*-test was calculated, \**P* < 0.05; \*\*\**P* < 0.001.

PHF8 proteins are located in the cell nucleus. (Supplementary Figure S5E).

Altogether, these data suggest that PHF8 phosphorylation is likely the major effect of ERK2 on PHF8. This event could regulate PHF8 affinity to the IFN $\gamma$ -responsive promoters, facilitating its eviction upon signaling.

## DISCUSSION

In this paper, we demonstrate a new role of PHF8 in controlling the precise response of IFN $\gamma$  signaling. We provide evidence for an H4K20me1 methylation/demethylation mechanism, mediated by PHF8, involved in the IFN $\gamma$  response. Our data indicate that prior to IFN $\gamma$  signaling, PHF8 is bound to a subset of IFN $\gamma$ -responsive promoters and,

through association with corepressors such as HDAC1 and SIN3A, PHF8 keeps these promoters in an inactive state, maintaining H4K20me1 at low levels (Figure 2). Upon IFN $\gamma$  treatment, PHF8 is phosphorylated by ERK2 and evicted from the promoters, which correlates with an increase in H4K20me1 and H3K4me3 levels. Our results strongly indicate that in addition to its well-characterized function as a coactivator (59), PHF8 could be silencing transcription to allow an accurate response.

Although the best-known role for PHF8 is the cooperation in gene activation, there are indeed some data in the literature that suggest a possible contribution of PHF8 to the silencing of transcription:



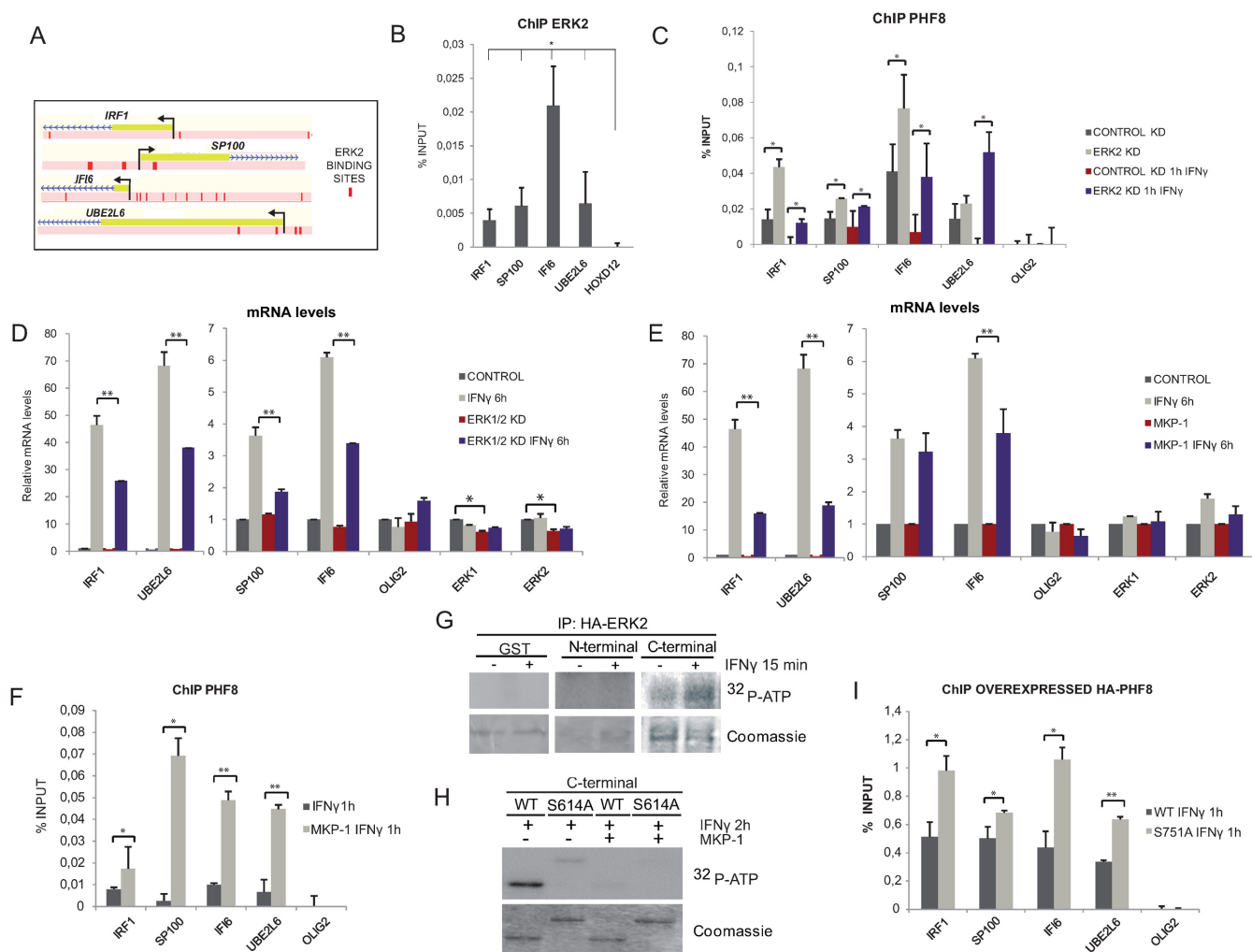


**Figure 4.** ERK2 regulates PHF8's chromatin binding affinity. (A) Evolutionary Conserved Regions online tool capture showing the presence of the ERK2 binding sites at the IFN $\gamma$  responsive promoters. (B) ERK2 ChIP assay analyzed by qPCR at the TSS of the indicated genes in HeLa S3 cells. (C) PHF8 ChIP assay in HeLa S3 CONTROL and ERK2 KD cells prior and upon IFN $\gamma$  stimulation (1h) analyzed by qPCR at the TSS of the indicated genes. Percentage of input represents the mean of at least three biological independent experiments. Error bars indicate S.E.M. For statistical analysis a paired-sample *t*-test was calculated,  $*P < 0.05$ . (D) mRNA levels of several PHF8-dependent and IFN $\gamma$ -responsive genes in HeLa S3 CONTROL and ERK1/2 KD cells prior and upon IFN $\gamma$  stimulation (6h) quantified by qPCR. Data were normalized by 18S mRNA levels. Results are the mean of three biological independent experiments. Error bars indicate S.E.M. For statistical analysis a paired-sample *t*-test was calculated,  $*P < 0.05$ ;  $**P < 0.01$ . (E) Total mRNA from HeLa cells overexpressing or not MKP-1 was prepared. The mRNA levels of several PHF8-dependent and IFN $\gamma$ -responsive genes were evaluated by qPCR prior and upon IFN $\gamma$  stimulation. qPCR raw values were normalized to 18S mRNA. Results depict a representative experiment from the three independent biological replicates. Error bars indicate S.E.M. of technical triplicates. For statistical analysis a paired-sample *t*-test was calculated,  $*P < 0.05$ ;  $**P < 0.01$ . (F) PHF8 ChIP assay in HeLa cells overexpressing or not MKP-1 upon IFN $\gamma$  stimulation (1h) analyzed by qPCR at the TSS of the indicated genes. Percentage of input represents the mean of at least two biological independent experiments. Error bars indicate S.E.M. For statistical analysis a paired-sample *t*-test was calculated,  $*P < 0.05$ ;  $**P < 0.01$ . (G) ERK2 purified from 293T cells overexpressing stimulated or not with IFN $\gamma$  (15 min) was used in a kinase assay with the GST, GST-mPHF8 N-terminus and GST-mPHF C-terminus. Top panel corresponds to the  $^{32}$ P-ATP signals and the bottom panel to Coomassie staining of the GST proteins used in the assay. The figure shown is representative of at least three biological independent experiments. (H) ERK2 purified from 293T cells stimulated with IFN $\gamma$  (2h) and overexpressing or not MKP-1 was used in a kinase assay with the GST-mPHF8 C-terminus WT or mutated at serine 614 to alanine (S614A). Top panel corresponds to the  $^{32}$ P-ATP signals and the bottom panel to Coomassie staining of the GST proteins used in the assay. The figure shown is representative of at least three biological independent experiments. (I) hPHF8-HA WT or hPHF8-HA mutated at serine 751 to alanine [PHF8 (S751A)] were transfected into HeLa S3 cells. ChIP assays were performed using the HA antibody upon IFN $\gamma$  stimulation (1h) and the PHF8 binding to the indicated promoters was analyzed by qPCR. Percentage of input represents the mean of at least two biological independent experiments. Error bars indicate S.E.M. For statistical analysis a paired-sample *t*-test was calculated,  $*P < 0.05$ ;  $**P < 0.01$ .

- i. Recently, through bioinformatic analysis, PHF8 has been shown to co-localize with the corepressor REST/NSRF. Furthermore, the authors suggest a potentially repressive role of these epigenetic regulators (17,35).
- ii. PHF8 demethylates H4K20me1. This marker has been historically associated with transcriptional repression (16,65). However, data published by several other groups indicate that it is involved in transcriptional activation (34,66–68). Moreover, H4K20me1 levels are strictly dependent on the cell cycle phase. These data suggest that PHF8, as the only enzyme responsible for H4K20me1 demethylation, might play a role as a corepressor in a spatial- and time-dependent manner.

Another histone marker related to IFN $\gamma$  signaling is H3K9me2. In their paper, Fang *et al.* demonstrated that enhanced levels of H3K9me2 are required to prevent an aberrant IFN response (62). Intriguingly, although this mark is removed by the HDM activity of PHF8 (28,32,52,61) and while we detected a clear increase in this histone modification upon IFN $\gamma$  addition, our PHF8 knockdown experiments demonstrate that this change is not dependent on PHF8 (Supplementary Figure S3F). Involvement of H3K9 methyltransferase G9A (62) or HDM members of KDM3, KDM4 or KDM7 families could explain this PHF8-independent effect. Everything considered, this evidence robustly suggests the possibility that PHF8 might contribute to fine-tuning transcription by maintaining the required balance of H4K20 methylation at the IFN $\gamma$ -responsive gene promoters, thus preventing signal-independent activation. Interestingly, it has been reported that PHF2, another member of the KDM7 family, might act as both a transcriptional corepressor of PolII and PolII regulated genes (66,69) and a coactivator of pro-inflammatory genes (14). In addition, it has recently been demonstrated that PHF8 and PHF2 compete *in vitro* for binding to H3K4me3 through their PHD domains (69). Thus, among the potential partners of PHF8 in the regulation of the IFN $\gamma$  genes, PHF2 could play a major role. It would be challenging to test whether these HDMs cooperate or compete to fine-tune the pro-inflammatory gene transcriptional response.

One still open question is related to the factor/s responsible for PHF8 targeting to these promoters. Data in the literature propose that ERK2 binds and represses these promoters by recognizing the sequence C/GAAAC/G (58). These data suggested that ERK2 could be mediating PHF8 recruitment to this subset of promoters. However, our ChIP experiments in ERK2 KD cells indicate that ERK2 is not responsible for PHF8 targeting to the IFN $\gamma$ -responsive promoters; the main role of ERK2 is to modulate the affinity of the PHF8-chromatin association (Figure 4). Furthermore, additional contributions of ERK2 to PHF8 function are also plausible, as has been suggested (63). Along with the chromatin-related role, ERK2 might possess other functions that facilitate IFN $\gamma$ -induced transcriptional response independently of PHF8. Curiously, it has been shown that ERK2 phosphorylates H3S10 in response to LPS at the *IL-10* gene, increasing SP1 binding to the promoter (70). Moreover, ERK1/2 phosphorylates RNA Pol II to activate transcription in ESCs (71) and facilitates activation by releasing

the SIN3A–HDAC complex from Sp1 binding sites at the *LHR* promoter in HeLa cells (72). Finally, IFN $\gamma$  recruits RNA Pol II to the *TNF* promoter via ERK signaling, without initiating transcription, leading to a paused state (73).

PHF8 is an essential protein for neural development and in particular, for induction of neural differentiation (74) and acquisition of the proper neuronal morphology (21). Moreover, PHF8 mutations are associated with X-linked mental retardation and ASDs (22–27). A close relation between mental illness, specifically ASDs and neuroinflammation has been clearly established. Several studies have shown that inflammatory cytokines are elevated in blood mononuclear cells, serum, plasma and cerebrospinal fluid of autistic subjects (75–78). As our findings suggests that PHF8-mediated H4K20me1 demethylation contributes to silencing genes involved in the inflammatory response, it would be interesting to test whether modulation of PHF8 activity alleviates ASDs symptoms, thus potentially constituting a novel approach for the treatment of inflammatory diseases.

## SUPPLEMENTARY DATA

Supplementary Data are available at NAR Online.

## ACKNOWLEDGEMENTS

We would like to thank Dr Christoph Loenarz for the HA-PHF8 vector, Dr Bob Eisenman for the pCS2+MT-mSin3A vector, Dr John Blenis for the pcDNA3-HA-ERK2 WT vector and Drs Pura Muñoz and Eusebio Perdiguero for the pSG5-MKP-1 vector. We also thank Dr J Roig for technical assistance and helpful discussions.

## FUNDING

Spanish MINECO [BFU2009-11527, BFU-2012-34261 to M.A.M.B.; BFU2009-11527, BIO2006-15557 to X.C.]; Fundació La Marató de TV3 [090210 to M.A.M.B.]; Fondation Jérôme Lejeune (to M.A.M.B.); Consejo Superior Investigaciones Científicas [200420E578 to X.C.]; FPU Fellowship (to R.F.). Funding for open access charge: Spanish MINECO [BFU2015-69248].

*Conflict of interest statement.* None declared.

## REFERENCES

1. Kawai,T. and Akira,S. (2010) The role of pattern-recognition receptors in innate immunity: update on Toll-like receptors. *Nat. Immunol.*, **11**, 373–384.
2. Takeuchi,O. and Akira,S. (2010) Pattern recognition receptors and inflammation. *Cell*, **140**, 805–820.
3. Lemaitre,B. and Hoffmann,J. (2007) The host defense of *Drosophila melanogaster*. *Annu. Rev. Immunol.*, **25**, 697–743.
4. Martinelli,C. and Reichhart,J.M. (2005) Evolution and integration of innate immune systems from fruit flies to man: lessons and questions. *J. Endotoxin. Res.*, **11**, 243–248.
5. Darnell,J.E. Jr (1997) STATs and gene regulation. *Science*, **277**, 1630–1635.
6. Hotamisligil,G.S. (2006) Inflammation and metabolic disorders. *Nature*, **444**, 860–867.
7. Tedgui,A. and Mallat,Z. (2006) Cytokines in atherosclerosis: pathogenic and regulatory pathways. *Physiol. Rev.*, **86**, 515–581.
8. Glass,C.K., Saijo,K., Winner,B., Marchetto,M.C. and Gage,F.H. (2010) Mechanisms underlying inflammation in neurodegeneration. *Cell*, **140**, 918–934.

9. Ogawa,S., Lozach,J., Jepsen,K., Sawka-Verhelle,D., Perissi,V., Sasik,R., Rose,D.W., Johnson,R.S., Rosenfeld,M.G. and Glass,C.K. (2004) A nuclear receptor corepressor transcriptional checkpoint controlling activator protein 1-dependent gene networks required for macrophage activation. *Proc. Natl. Acad. Sci. U.S.A.*, **101**, 14461–14466.
10. Ghisletti,S., Huang,W., Jepsen,K., Benner,C., Hardiman,G., Rosenfeld,M.G. and Glass,C.K. (2009) Cooperative NCoR/SMRT interactions establish a corepressor-based strategy for integration of inflammatory and anti-inflammatory signaling pathways. *Genes Dev.*, **23**, 681–693.
11. Hargreaves,D.C., Horng,T. and Medzhitov,R. (2009) Control of inducible gene expression by signal-dependent transcriptional elongation. *Cell*, **138**, 129–145.
12. Hoberg,J.E., Yeung,F. and Mayo,M.W. (2004) SMRT derepression by the IkappaB kinase alpha: a prerequisite to NF-kappaB transcription and survival. *Mol. Cell*, **16**, 245–255.
13. Pascual,G., Fong,A.L., Ogawa,S., Gamlie,A., Li,A.C., Perissi,V., Rose,D.W., Willson,T.M., Rosenfeld,M.G. and Glass,C.K. (2005) A SUMOylation-dependent pathway mediates transrepression of inflammatory response genes by PPAR-gamma. *Nature*, **437**, 759–763.
14. Stender,J.D., Pascual,G., Liu,W., Kaikkonen,M.U., Do,K., Spann,N.J., Boutros,M., Perimon,N., Rosenfeld,M.G. and Glass,C.K. (2012) Control of proinflammatory gene programs by regulated trimethylation and demethylation of histone H4K20. *Mol. Cell*, **48**, 28–38.
15. Jorgensen,S., Schotta,G. and Sorensen,C.S. (2013) Histone H4 lysine 20 methylation: key player in epigenetic regulation of genomic integrity. *Nucleic Acids Res.*, **41**, 2797–2806.
16. Beck,D.B., Oda,H., Shen,S.S. and Reinberg,D. (2012) PR-Set7 and H4K20me1: at the crossroads of genome integrity, cell cycle, chromosome condensation, and transcription. *Genes Dev.*, **26**, 325–337.
17. Liu,W., Tanasa,B., Tyurina,O.V., Zhou,T.Y., Gassmann,R., Liu,W.T., Ohgi,K.A., Benner,C., Garcia-Bassets,I., Aggarwal,A.K. *et al.* (2010) PHF8 mediates histone H4 lysine 20 demethylation events involved in cell cycle progression. *Nature*, **466**, 508–512.
18. Fortschegger,K. and Shiekhhattar,R. (2011) Plant homeodomain fingers form a helping hand for transcription. *Epigenetics*, **6**, 4–8.
19. Lim,H.J., Dimova,N.V., Tan,M.K., Sigoillot,F.D., King,R.W. and Shi,Y. (2013) The G2/M regulator histone demethylase PHF8 is targeted for degradation by the anaphase-promoting complex containing CDC20. *Mol. Cell Biol.*, **33**, 4166–4180.
20. Yatim,A., Benne,C., Sobhian,B., Laurent-Chabalier,S., Deas,O., Judde,J.G., Lelievre,J.D., Levy,Y. and Benkirane,M. (2012) NOTCH1 nuclear interactome reveals key regulators of its transcriptional activity and oncogenic function. *Mol. Cell*, **48**, 445–458.
21. Asensio-Juan,E., Gallego,C. and Martinez-Balbas,M.A. (2012) The histone demethylase PHF8 is essential for cytoskeleton dynamics. *Nucleic Acids Res.*, **40**, 9429–9440.
22. Siderius,L.E., Hamel,B.C., van Bokhoven,H., de Jager,F., van den Helm,B., Kremer,H., Heineman-de Boer,J.A., Ropers,H.H. and Mariman,E.C. (1999) X-linked mental retardation associated with cleft lip/palate maps to Xp11.3-q21.3. *Am. J. Med. Genet.*, **85**, 216–220.
23. Abidi,F.E., Miano,M.G., Murray,J.C. and Schwartz,C.E. (2007) A novel mutation in the PHF8 gene is associated with X-linked mental retardation with cleft lip/cleft palate. *Clin. Genet.*, **72**, 19–22.
24. Koivisto,A.M., Ala-Mello,S., Lemmela,S., Komu,H.A., Rautio,J. and Jarvela,I. (2007) Screening of mutations in the PHF8 gene and identification of a novel mutation in a Finnish family with XLMR and cleft lip/cleft palate. *Clin. Genet.*, **72**, 145–149.
25. Laumonier,F., Holbert,S., Ronce,N., Faravelli,F., Lenzner,S., Schwartz,C.E., Lespinasse,J., Van Esch,H., Lacombe,D., Goizet,C. *et al.* (2005) Mutations in PHF8 are associated with X linked mental retardation and cleft lip/cleft palate. *J. Med. Genet.*, **42**, 780–786.
26. Nava,C., Lamari,F., Heron,D., Mignot,C., Rastetter,A., Keren,B., Cohen,D., Faudet,A., Bouteiller,D., Gilleron,M. *et al.* (2012) Analysis of the chromosome X exome in patients with autism spectrum disorders identified novel candidate genes, including TMLHE. *Transl. Psychiatry*, **2**, e179.
27. Fueyo,R., Garcia,M.A. and Martinez-Balbas,M.A. (2015) Jumonji family histone demethylases in neural development. *Cell Tissue Res.*, **359**, 87–98.
28. Kleine-Kohlbrecher,D., Christensen,J., Vandamme,J., Abarrategui,I., Bak,M., Tommerup,N., Shi,X., Gozani,O., Rappsilber,J., Salcini,A.E. *et al.* (2010) A functional link between the histone demethylase PHF8 and the transcription factor ZNF711 in X-linked mental retardation. *Mol. Cell*, **38**, 165–178.
29. Fortschegger,K., de Graaf,P., Outchkourov,N.S., van Schaik,F.M., Timmers,H.T. and Shiekhhattar,R. (2010) PHF8 targets histone methylation and RNA polymerase II to activate transcription. *Mol. Cell Biol.*, **30**, 3286–3298.
30. Tsukada,Y., Ishitani,T. and Nakayama,K.I. (2010) KDM7 is a dual demethylase for histone H3 Lys 9 and Lys 27 and functions in brain development. *Genes Dev.*, **24**, 432–437.
31. Wen,H., Li,J., Song,T., Lu,M., Kan,P.Y., Lee,M.G., Sha,B. and Shi,X. (2010) Recognition of histone H3K4 trimethylation by the plant homeodomain of PHF2 modulates histone demethylation. *J. Biol. Chem.*, **285**, 9322–9326.
32. Horton,J.R., Upadhyay,A.K., Qi,H.H., Zhang,X., Shi,Y. and Cheng,X. (2010) Enzymatic and structural insights for substrate specificity of a family of jumonji histone lysine demethylases. *Nat. Struct. Mol. Biol.*, **17**, 38–43.
33. Lois,S., Akizu,N., de Xaxars,G.M., Vazquez,I., Martinez-Balbas,M. and de la Cruz,X. (2010) Characterization of structural variability sheds light on the specificity determinants of the interaction between effector domains and histone tails. *Epigenetics*, **5**, 137–148.
34. Li,Z., Nie,F., Wang,S. and Li,L. (2011) Histone H4 Lys 20 monomethylation by histone methylase SET8 mediates Wnt target gene activation. *Proc. Natl. Acad. Sci. U.S.A.*, **108**, 3116–3123.
35. Wang,J., Lin,X., Wang,S., Wang,C., Wang,Q., Duan,X., Lu,P., Liu,X.S. and Huang,J. (2014) PHF8 and REST/NRSF co-occupy gene promoters to regulate proximal gene expression. *Sci. Rep.*, **4**, 5008.
36. Blanco-Garcia,N., Asensio-Juan,E., de la Cruz,X. and Martinez-Balbas,M.A. (2009) Autoacetylation regulates P/CAF nuclear localization. *J. Biol. Chem.*, **284**, 1343–1352.
37. Akizu,N., Estaras,C., Guerrero,L., Marti,E. and Martinez-Balbas,M.A. (2010) H3K27me3 regulates BMP activity in developing spinal cord. *Development*, **137**, 2915–2925.
38. Valls,E., Blanco-Garcia,N., Aquizu,N., Piedra,D., Estaras,C., de la Cruz,X. and Martinez-Balbas,M.A. (2007) Involvement of chromatin and histone deacetylation in SV40 T antigen transcription regulation. *Nucleic Acids Res.*, **35**, 1958–1968.
39. Slack,D.N., Seternes,O.M., Gabrielsen,M. and Keyse,S.M. (2001) Distinct binding determinants for ERK2/p38alpha and JNK map kinases mediate catalytic activation and substrate selectivity of map kinase phosphatase-1. *J. Biol. Chem.*, **276**, 16491–16500.
40. Dimitri,C.A., Dowdle,W., MacKeigan,J.P., Blenis,J. and Murphy,L.O. (2005) Spatially separate docking sites on ERK2 regulate distinct signaling events in vivo. *Curr. Biol.*, **15**, 1319–1324.
41. Sanchez-Molina,S., Oliva,J.L., Garcia-Vargas,S., Valls,E., Rojas,J.M. and Martinez-Balbas,M.A. (2006) The histone acetyltransferases CBP/p300 are degraded in NIH 3T3 cells by activation of Ras signalling pathway. *Biochem. J.*, **398**, 215–224.
42. Sanchez-Molina,S., Estaras,C., Oliva,J.L., Akizu,N., Asensio-Juan,E., Rojas,J.M. and Martinez-Balbas,M.A. (2014) Regulation of CBP and Tip60 coordinates histone acetylation at local and global levels during Ras-induced transformation. *Carcinogenesis*, **35**, 2194–2202.
43. Valls,E., Sanchez-Molina,S. and Martinez-Balbas,M.A. (2005) Role of histone modifications in marking and activating genes through mitosis. *J. Biol. Chem.*, **280**, 42592–42600.
44. ENCODE Project Consortium (2012) An integrated encyclopedia of DNA elements in the human genome. *Nature*, **489**, 57–74.
45. Goecks,J., Nekrutenko,A. and Taylor,J. (2010) Galaxy: a comprehensive approach for supporting accessible, reproducible, and transparent computational research in the life sciences. *Genome Biol.*, **11**, R86–R98.
46. Trapnell,C., Pachter,L. and Salzberg,S.L. (2009) TopHat: discovering splice junctions with RNA-Seq. *Bioinformatics*, **25**, 1105–1111.
47. Trapnell,C., Williams,B.A., Pertea,G., Mortazavi,A., Kwan,G., van Baren,M.J., Salzberg,S.L., Wold,B.J. and Pachter,L. (2010) Transcript assembly and quantification by RNA-Seq reveals unannotated



- transcripts and isoform switching during cell differentiation. *Nat. Biotechnol.*, **28**, 511–515.
48. Trapnell, C., Hendrickson, D.G., Sauvageau, M., Goff, L., Rinn, J.L. and Pachter, L. (2013) Differential analysis of gene regulation at transcript resolution with RNA-seq. *Nat. Biotechnol.*, **31**, 46–53.
  49. Puig, O., Caspary, F., Rigaut, G., Rutz, B., Bouveret, E., Bragado-Nilsson, E., Wilm, M. and Seraphin, B. (2001) The tandem affinity purification (TAP) method: a general procedure of protein complex purification. *Methods*, **24**, 218–229.
  50. Estaras, C., Akizu, N., Garcia, A., Beltran, S., de la Cruz, X. and Martinez-Balbas, M.A. (2012) Genome-wide analysis reveals that Smad3 and JMJD3 HDM co-activate the neural developmental program. *Development*, **139**, 2681–2691.
  51. Caelles, C. and Morales, M. (2004) Assays to measure stress-activated MAPK activity. *Methods Mol. Biol.*, **282**, 145–156.
  52. Qi, H.H., Sarkissian, M., Hu, G.Q., Wang, Z., Bhattacharjee, A., Gordon, D.B., Gonzales, M., Lan, F., Ongusaha, P.P., Huarte, M. *et al.* (2010) Histone H4K20/H3K9 demethylase PHF8 regulates zebrafish brain and craniofacial development. *Nature*, **466**, 503–507.
  53. Ng, H.H. and Bird, A. (2000) Histone deacetylases: silencers for hire. *Trends Biochem. Sci.*, **25**, 121–126.
  54. Ayer, D.E. (1999) Histone deacetylases: transcriptional repression with SINers and NuRDs. *Trends Cell Biol.*, **9**, 193–198.
  55. Murphy, M., Ahn, J., Walker, K.K., Hoffman, W.H., Evans, R.M., Levine, A.J. and George, D.L. (1999) Transcriptional repression by wild-type p53 utilizes histone deacetylases, mediated by interaction with mSin3a. *Genes Dev.*, **13**, 2490–2501.
  56. Zhang, Y. and Dufau, M.L. (2004) Gene silencing by nuclear orphan receptors. *Vitam. Horm.*, **68**, 1–48.
  57. Feng, D., Sangster-Guity, N., Stone, R., Korczyńska, J., Mancl, M.E., Fitzgerald-Bocarsly, P. and Barnes, B.J. (2010) Differential requirement of histone acetylase and deacetylase activities for IRF5-mediated proinflammatory cytokine expression. *J. Immunol.*, **185**, 6003–6012.
  58. Hu, S., Xie, Z., Onishi, A., Yu, X., Jiang, L., Lin, J., Rho, H.S., Woodard, C., Wang, H., Jeong, J.S. *et al.* (2009) Profiling the human protein-DNA interactome reveals ERK2 as a transcriptional repressor of interferon signaling. *Cell*, **139**, 610–622.
  59. Suganuma, T. and Workman, J.L. (2010) Features of the PHF8/KIAA1718 histone demethylase. *Cell Res.*, **20**, 861–862.
  60. Ashburner, M., Ball, C.A., Blake, J.A., Botstein, D., Butler, H., Cherry, J.M., Davis, A.P., Dolinski, K., Dwight, S.S., Eppig, J.T. *et al.* (2000) Gene ontology: tool for the unification of biology. The Gene Ontology Consortium. *Nat. Genet.*, **25**, 25–29.
  61. Zhu, Z., Wang, Y., Li, X., Xu, L., Wang, X., Sun, T., Dong, X., Chen, L., Mao, H., Yu, Y. *et al.* (2010) PHF8 is a histone H3K9me2 demethylase regulating rRNA synthesis. *Cell Res.*, **20**, 794–801.
  62. Fang, T.C., Schaefer, U., Mecklenbrauker, I., Stienen, A., Dewell, S., Chen, M.S., Rioja, I., Parravicini, V., Prinjha, R.K., Chandwani, R. *et al.* (2012) Histone H3 lysine 9 di-methylation as an epigenetic signature of the interferon response. *J. Exp. Med.*, **209**, 661–669.
  63. Goke, J., Chan, Y.S., Yan, J., Vingron, M. and Ng, H.H. (2013) Genome-wide kinase-chromatin interactions reveal the regulatory network of ERK signaling in human embryonic stem cells. *Mol. Cell*, **50**, 844–855.
  64. Sun, L., Huang, Y., Wei, Q., Tong, X., Cai, R., Nalepa, G. and Ye, X. (2015) Cyclin E-CDK2 protein phosphorylates plant homeodomain finger protein 8 (PHF8) and regulates its function in the cell cycle. *J. Biol. Chem.*, **290**, 4075–4085.
  65. Wang, Y. and Jia, S. (2009) Degrees make all the difference: the multifunctionality of histone H4 lysine 20 methylation. *Epigenetics*, **4**, 273–276.
  66. Barski, A., Cuddapah, S., Cui, K., Roh, T.Y., Schones, D.E., Wang, Z., Wei, G., Chepelev, I. and Zhao, K. (2007) High-resolution profiling of histone methylations in the human genome. *Cell*, **129**, 823–837.
  67. Vakoc, C.R., Sachdeva, M.M., Wang, H. and Blobel, G.A. (2006) Profile of histone lysine methylation across transcribed mammalian chromatin. *Mol. Cell Biol.*, **26**, 9185–9195.
  68. Talasz, H., Lindner, H.H., Sarg, B. and Helliger, W. (2005) Histone H4-lysine 20 monomethylation is increased in promoter and coding regions of active genes and correlates with hyperacetylation. *J. Biol. Chem.*, **280**, 38814–38822.
  69. Shi, G., Wu, M., Fang, L., Yu, F., Cheng, S., Li, J., Du, J.X. and Wong, J. (2014) PHD finger protein 2 (PHF2) represses ribosomal RNA gene transcription by antagonizing PHF finger protein 8 (PHF8) and recruiting methyltransferase SUV39H1. *J. Biol. Chem.*, **289**, 29691–29700.
  70. Zhang, X., Edwards, J.P. and Mosser, D.M. (2006) Dynamic and transient remodeling of the macrophage IL-10 promoter during transcription. *J. Immunol.*, **177**, 1282–1288.
  71. Tee, W.W., Shen, S.S., Oksuz, O., Narendra, V. and Reinberg, D. (2014) Erk1/2 activity promotes chromatin features and RNAPII phosphorylation at developmental promoters in mouse ESCs. *Cell*, **156**, 678–690.
  72. Liao, M., Zhang, Y. and Dufau, M.L. (2008) Protein kinase Calpha-induced derepression of the human luteinizing hormone receptor gene transcription through ERK-mediated release of HDAC1/Sin3A repressor complex from Sp1 sites. *Mol. Endocrinol.*, **22**, 1449–1463.
  73. Garrett, S., Dietzmann-Maurer, K., Song, L. and Sullivan, K.E. (2008) Polarization of primary human monocytes by IFN-gamma induces chromatin changes and recruits RNA Pol II to the TNF-alpha promoter. *J. Immunol.*, **180**, 5257–5266.
  74. Qiu, J., Shi, G., Jia, Y., Li, J., Wu, M., Dong, S. and Wong, J. (2010) The X-linked mental retardation gene PHF8 is a histone demethylase involved in neuronal differentiation. *Cell Res.*, **20**, 908–918.
  75. Molloy, C.A., Morrow, A.L., Meinzen-Derr, J., Schleifer, K., Dienger, K., Manning-Courtney, P., Altaye, M. and Wills-Karp, M. (2006) Elevated cytokine levels in children with autism spectrum disorder. *J. Neuroimmunol.*, **172**, 198–205.
  76. El-Ansary, A.K., Ben Bacha, A.G. and Al-Ayadi, L.Y. (2011) Proinflammatory and proapoptotic markers in relation to mono and di-cations in plasma of autistic patients from Saudi Arabia. *J. Neuroinflammation*, **8**, 142–150.
  77. Chez, M.G., Burton, Q., Dowling, T., Chang, M., Khanna, P. and Kramer, C. (2007) Memantine as adjunctive therapy in children diagnosed with autistic spectrum disorders: an observation of initial clinical response and maintenance tolerability. *J. Child Neurol.*, **22**, 574–579.
  78. Croonenberghs, J., Bosmans, E., Deboutte, D., Kenis, G. and Maes, M. (2002) Activation of the inflammatory response system in autism. *Neuropsychobiology*, **45**, 1–6.